Plant and Crop Protection / Sanidad Vegetal y Producción de Cultivos

doi: http:// dx.doi.org/10.15446/acag.v64n3.42657 e-ISSN 2323-0118

Methodology for pest damage recognition in *Begonia semperflorens* link & Otto (sugar flower) crop through image processing

Procesamiento de imágenes para reconocimiento de daños causados por plagas en el cultivo de *Begonia semperflorens* Link & Otto (flor de azúcar)

Camilo Andrés Cáceres Flórez*, Darío Amaya Hurtado and Olga Lucía Ramos Sandoval

Faculty of Engineering. GAV Group. Universidad Militar Nueva Granada, Bogotá, Colombia.
*Corresponding author: u1801466@unimilitar.edu.co

Rec.: 13.03.2014 Acep.:06.06.2014

Abstract

Nowadays, an important element in farming, is the use of technology based on the analysis of the different factors that affect the successful development of the crops. In this work a computer machine vision as a diagnostic tool was used in the recognition of pests. The captured images were done with a drone, equipped with a camera for capturing images of the crop status of a plant called 'Flor de azúcar' (*Begonia semperflorens*). These images were processed using machine vision techniques to identify the possible attack of pests on the crop. The techniques used are morphological filters, Gaussian blur filter and HSL. The main result of this work was accomplished by detection of the perforation of the leaves as a result of pest attack, specifically slugs, snails, spider mites and leafminers.

Key words: Image processing, pest detection, farming monitoring, morphological filters, Gaussian Blur

Resumen

En este trabajo se presentan los resultados obtenidos en el reconocimiento de plagas utilizando la visión de máquina por computador como elemento de diagnóstico. La captura de las imágenes se realizó por medio de un agente robótico aéreo (drone) equipado con una cámara, lo que permitió capturar las imágenes del estado de las hojas de un cultivo de la planta conocida como 'flor de azúcar' (*Begonia semperflorens*). Estas imágenes fueron procesadas utilizando técnicas de visión de máquina con el fin de identificar el posible ataque de plagas en el cultivo. Las técnicas utilizadas corresponden a filtros morfológicos, difuminado gaussiano y filtrado HSL. Como resultado principal de este trabajo se detectaron perforaciones de hojas ocasionadas por el ataque de plagas, específicamente babosas, caracoles, arañas rojas y minadoras.

Palabras clave: Procesamiento de imágenes, detección de plagas, monitoreo de cultivos, filtros morfológicos, difuminado gaussiano.

Introduction

Digital processing of images is a widely used tool to automate industrial processes, since it is trustable, efficient and fast in the processing. The agricultural industry have begun to use this type of technology to monitor relevant aspects of the crops (Yan *et al.*, 2009; Noda *et al.*, 2006; and Husin *et al.*, 2012). In this paper the observations were made in growing *Begonia semperflorens* known as 'sugar flower' an ornamental plant that typically grows in warm, humid weather.

According to Fonterlz (2013) and Grbíc (2011) this plant is attacked by slugs, snails, spider mites and leafminers. The damage can be visually detected due to the holes left on the plant leaves, which is why it is possible to use machine vision to verify the level of damage. Specifically, for digital image processing filters for image segmentation can be used, including morphological filters. These filters are based on the shapes present on the images and tend to simplify the data in them, preserving the essential characteristics of the shape and eliminating the irrelevant ones (Barata and Pina, 2003; Najman *et al.*, 2010). The dilation technique is a morphological transformation that uses a vector addition to combine two sets of elements (Shih, 2009; Najman *el al.* 2010).

Gaussian blur is another algorithm used, its goal is to blend or smooth an image with a Gaussian function. It is generally used to reduce the digital noise and the details in the images. Several times this technique is used as an initial step in the processing of images obtained by machine vision, since this allows the elimination of the digital noise avoiding the loss of important information of the image (Nixon and Aguado, 2002; Gedraite and Hadad, 2011).

An additional method is the Hue Saturación Luminace (HSL) image filter. This is based on a color representation in polar coordinates, which is more natural that RGB representations because it is closer to the physiological perception of color by human eye (Etxeberria, 2010). This model defines the color space in three characteristics: Hue, Saturation and Luminance. The main advantage of a HSL filter on image processing is the robustness that it has under lightning changes (Jin–liang *et al.* 2008; Wesolkowski, 1999).

In image processing for recognition of pest and plant morphology, there are studies like the one of Yan *et al.* (2009) who proposed a new method to detect pests and automate the application of pesticides in greenhouse crops. The difference in color in the leaves of affected and healthy plants is determined by means of image segmentation to identify the possible pests. The results are used by a robot that goes around the greenhouse applying the pesticide where the pest identification indicates. This method is called

This method is based on triangulation and binocular vision to calculate the 3D position of the plant. The research by Noda *et al.* (2006) are intended to control peripheral devices, based on the features extracted from the images acquired by a field server used in industrial applications; these researchers were able to detect the degree of wilting of the plant using image processing methods. Husin *et al.* (2012) proposed early detection of pests affecting pepper plants through the inspection of the characteristics of the leaves or the stem, using image processing with RGB color model, which allows to extract the captured images and the sections corresponding to pepper leaves to identify, through grouping of colors, those leaves that show signs of disease or are attacked by pests.

This research has as objective to implement a system for pest recognition in 'sugar flower' (*Begonia semperflorens*) crop through image processing. This plant was selected mainly for the easiness of image acquisition and touring of the crop with a drone type robot. The contribution of this work lies in the quantitative analysis of the damage produced in a plant by pests and the use of unmanned aerial robot to capture images.

Materials and methods

Location of the crop and image acquisition

To develop this work, initially, an image capturing was done in the first week of June, 2013 in the city of Bogota, 4° 40' 59.07" N and 74° 2' 30.94" W, on a small crop of ornamental flowers of *B. semperflorens*. Image capturing was done between 9 to 11 a.m., with an approximate temperature of 17.7 °C, on a sunny non-cloudy day. Pictures were taken using an aerial robot (AR) 'Quadcopter', AR Drone 2.0 (Developed by Parrot, model 2.0) which has a high definition (HD) frontal camera of 720 pixels and 30 photograms per second. In addition to the frontal camera, the AR has a bottom camera with 640 x 480 pixels resolution that was used

to get additional images of the crop.

For this research 200 pictures were taken in different positions. With the front camera 100 photographs were captured and with the bottom camera a similar number was captured. 10 photos were captured every 5 cm, starting at 5 cm and ending at 55 cm. The first 100 pictures were taken with the bottom camera perpendicular to the ground. The 100 photographs taken with the front camera had a tilt angle of 30° between the ground and the AR.

Image capturing and processing

Images were subjected to an off-line process, on a software developed in Visual Express C#2010 using the open source AForge.net library, this library facilitates image processing and artificial intelligence techniques. The developed software is totally automated, takes the images from the AR and analyzes them in a serial basis. The results of the analysis can be seen in the software while the image analysis is running, additionally it saves a record in Excel sheets with the name of the analyzed image and the result of the analysis.

The procedure involved applying different types of filters to the obtained images. The application of these filters was made in order to observe the damaged parts of the leaf and quantify them computationally according to the percentage of damage. Figure 1 shows an image of Parrot AR Drone 2.0 and a photo taken by RA at a distance of 30 cm from the plant.

Figure 1. ARDrone 2.0 in front of the target crop (Crop picture taken by the Drone).

The basic requirement of the algorithm is pattern recognition reflected in holes in the leaves of the plant. Due to the small size of these holes, it sought initially to use some kind of mathematical morphology to highlight those features. Subsequently, image smoothing was performed to reduce noise and increase the accuracy of the algorithm. In addition, a HSL filter, which is very robust in color separation was applied, and was thresholding; lastly the location of the holes with respect to the leaf was analyzed through binary multidimensional arrays. In Figure 2 a diagram of the developed algorithm is included.

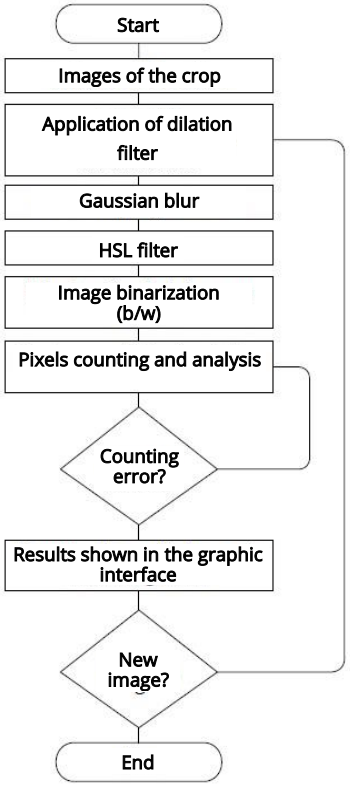

Figure 2. Diagram of the developed algorithm.

Application of the morphological dilation filter

Initially, an algorithm that would highlight the characteristics of small holes that are intended to be recognized in the image was searched. This objective can be achieved through a type of mathematical morphology called 'dilation', which is described as growth pixels. This allows increasing one pixel around the circumference of each region and in that way the dimensions are increased. The same method was used in the work of Barata and Pina (2003). The function used is pre-determined in the AForge.net library and the dilation is given by the Equations 1 and 2. This means that the set of all possible vectors is the sum of the pair of elements, one belonging to A and other to B.

$$A \oplus B = \{a + b : a \in A \; y \; b \in B\} \qquad (1)$$

$$X \in A \oplus B \Leftrightarrow x = a + b, a \in A \; y \; b \in B \quad (2)$$

where, A and B are geometric structures of continuous or discrete space.

Application of Gaussian blur

After the application of dilation noise was still observed in the image and some other could be generated by the morphology filter (Hendriks *et al.*, 2013). This makes it necessary to smooth the image through the filtering process: in this case was used the 'Gaussian Blur', which is associated with the Equation 3 that follows, which corresponds to a Gaussian function representing a normal distribution in one dimension but in this specific case a normal distribution is required in two dimensions which is the product of two unidimensional Gaussian equations (Sun, 2012). In the Equation 4 the result is shown.

$$G(x) = \frac{1}{\sqrt{2\pi\sigma^2}} e^{-\frac{x^2}{2\sigma^2}} \quad (3)$$

$$G(x,y) = \frac{1}{\sqrt{2\pi\sigma^2}} e^{-\frac{x^2+y^2}{2\sigma^2}} \quad (4)$$

The Equation 4, corresponding to the Gaussian blur in two dimensions, depends on a sigma value (σ) that is the standard deviation of the Gaussian distribution. In this case, after analyzing different values, the chosen value was 1.5 to reduce the noise in the image (Perkins, 2009). Additionally, the y and x values refer to the position of the analyzed pixels. In Figure 3 is shown an application of the Gaussian Blur to the resulting image after dilation was applied.

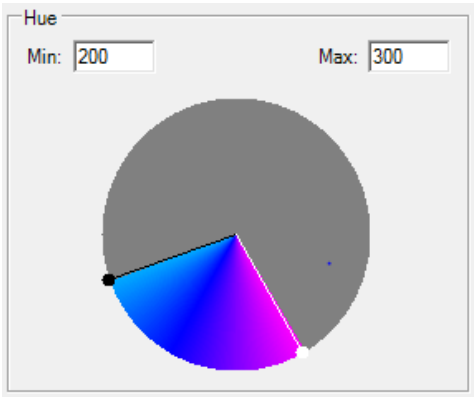

Figure 3. HSL range for Hue

Application of the HSL filter

With the smoothed image of Figure 4 the filtering is done, in order to get only the leaves of the plant, to calculate later the percentage of the leaf that is damaged. A HSL filter is used, because of its robustness and flexibility in contrast to the RGB filter, additionally it filters the color without any problem for light and shine as happens when the RGB filter is used (Bovik, 2005). For the filter values determined by the average values of the analyzed leaves are used. The used values for saturation were between 0.1 and 0.35, luminance between 0.15 and 0.4 and tint between 200 and 300, as shown in Figure 9 after applying the HSL filter to the Figure 5.

Figure 4. Resulting image after dilation and Gaussian blur filters.

Figure 5. Image of the figure 4 with HSL filter.

Application of binarization, data collection and analysis

Finally binarization was applied (Bovik, 2005) with the lowest threshold value to get a black and white image (Figure 6) and processing it in multidimensional arrangements.

Then, the image goes for a multidimensional array (matrix), with values of 1 (white) and 0 (black), in order to highlight the search for white areas (leaves) in which isolated or adja-

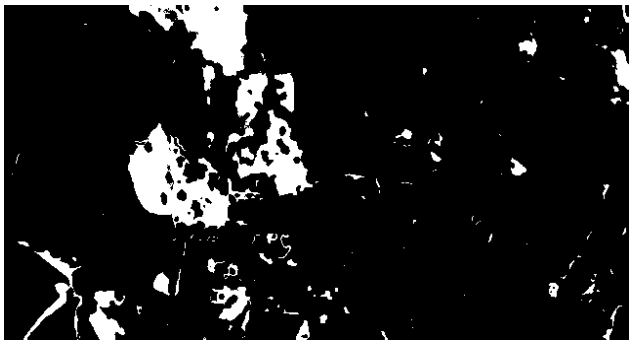

Figure 6. Binarized test image.

cent black pixels are looked for. Isolated black pixels on a white sector are associated with a hole left by a pest. If the black sector is not isolated is associated with a possible hole since it can be the shape of the leaf, a shape or a potential hole, it is uncertain and therefore the value of probability of a hole is indicated.

Once the entire image is scanned the area of the white zones corresponding to the leaf area without holes (white) is determined in pixels. Subsequently, the area of black pixels in the white areas is obtained, the black areas have at least four adjacent white pixels. The arithmetic mean of all black pixels is calculated in the white area as specified, which represents the percentage of the leaf with holes and subtracting it from 100%, the percentage of leaves without holes is obtained. These representations can be seen in Equations 5 and 6, respectively.

$$TAa = \frac{\sum_{i=0}^{An}\sum_{j=0}^{Al} Pn}{\sum_{i=0}^{An}\sum_{j=0}^{Al}(Pb+Pn)} \times 100\% \qquad (5)$$

$$TAna = \left(\frac{\sum_{i=0}^{An}\sum_{j=0}^{Al} Pn}{\sum_{i=0}^{An}\sum_{j=0}^{Al}(Pb+Pn)} - 1\right) \times 100\% \quad (6)$$

where, TAa is the percentage of the total area affected, $TAan$ is the percentage of the total area non-affected, An in the width of the image, Al is the high of the image, Pn is the number of black pixels with at least four white pixels on a surrounding area of 3 x 3 pixels, Pb is the number of white pixels, i and j are numbers that belong to the image scanning by the multidimensional array, a is the number of pixels in the image. These Equations 5 and 6 are general for the analysis of any size image.

On the other hand, the percentage of the leaf that is probably affected by the pest is taken as the fraction between black pixels with three or four adjacent white pixels, since it is not possible to determine whether the leaf blade is in good conditions, this uncertainty is left since it is not possible to calculate by the chosen algorithms. The applied model can be seen in the Equation 7.

$$TI = \frac{\sum_{i=0}^{An}(\sum_{j=0}^{Al} Pn2)}{\sum_{i=0}^{An}(\sum_{j=0}^{Al}(Pb+Pn))} \times 100\% \qquad (7)$$

where, TI is the percentage of total uncertainty over the leaf area, $Pn2$ is the number of black pixels with three or four adjacent white pixels on a 3 x 3 pixels area, the other variables are the same as in Equations 5 and 6.

Figure 7 corresponds to an example of a leaf (white area) with a hole (black area surrounded by a red circle) that shows graphically what is expressed in Equations 5 and 6. Figure 8 shows an example of a leaf (white area) with the probability of a hole (black area, surrounded by a red circle), that shows graphically what is expressed in the Equation 7. Finally, the Figure 9 shows an example of how the leaves were separated from the whole image (in white), without losing information of the hole on the leaf.

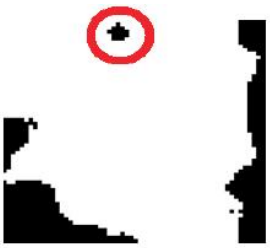

Figure 7. Observed hole.

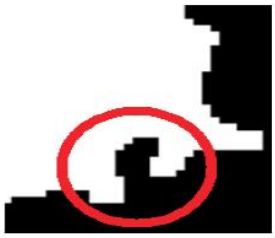

Figure 8. Probable hole.

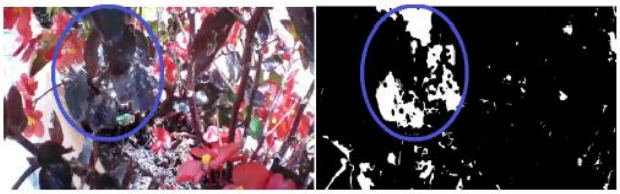

Figure 9. Initial image vs. filtered image (leaves are white color).

The algorithm thresholds were found by a supervised multilayer neuronal network that was used to find the optimal parameters for the different algorithm used. The use of such network after its testing with the 60% of the pictures taken was highly limited by the processing time required for the analysis of each image. The analysis of precision was based in comparing the optimal results found by the neuronal network used in this software and, the parameters found for each image in particular, which are more precise for each individual image but not for all the group of images. The error mean among the parameters found by the neuronal network and the individual one for each image was 9.8%, therefore, the certainty percentage was 90.2%.

Results and discussion

The main problem in the development of this project was the determination of the correct thresholds for each algorithm used, the solution consisted on optimizing the parameter of the algorithms by a supervised neuronal multilayer network. Such network was used as basis for the software analysis, its reliability and the corresponding analysis are shown in Table 1 and 2. The use of such network, after its testing with 60% of the taken images, which was highly limited by the processing time required for the analysis of each image due to the high number of layers used, therefore, it was used only as reference. In Tables 1 and 2 are included the efficiency based on the rate between the proposed method and the value obtained

Table 1. Results of the effectiveness for the camera with 640x480 resolution.

Distance (cm)	Efectiveness of the method (%)									
	Image 1	Image 2	Image 3	Image 4	Image 5	Image 6	Image 7	Image 8	Image 9	Image 10
5	67.60%	64.60%	71.90%	67.00%	62.60%	69.10%	71.80%	65.20%	65.80%	64.90%
10	60.60%	65.60%	64.80%	65.10%	58.60%	64.20%	59.60%	62.50%	64.60%	60.80%
15	52.10%	56.30%	56.20%	48.20%	57.10%	55.70%	51.40%	48.70%	50.30%	57.20%
20	43.40%	41.50%	45.70%	39.30%	45.40%	43.50%	45.20%	45.20%	42.40%	46.90%
25	39.80%	44.60%	36.30%	43.40%	35.80%	39.90%	40.00%	44.30%	38.80%	44.70%
30	37.90%	34.80%	41.20%	33.50%	41.90%	34.30%	42.10%	38.80%	42.20%	42.10%
35	30.30%	33.20%	29.30%	35.80%	33.30%	26.90%	31.20%	27.10%	32.10%	29.20%
40	25.60%	26.10%	23.50%	25.90%	21.60%	22.70%	20.20%	27.30%	25.50%	24.40%
45	20.90%	22.50%	17.60%	24.10%	21.90%	20.50%	23.60%	18.60%	20.80%	20.40%
50	15.70%	13.60%	10.40%	16.20%	16.70%	18.30%	18.80%	14.60%	12.20%	15.30%
55	11.10%	9.80%	10.20%	16.30%	6.10%	9.10%	15.90%	13.10%	14.30%	9.90%

Table 2. Results of the effectiveness for the HD 720p camera.

Distance (cm)	Effectiveness of the method (%)									
	Image 1	Image 2	Image 3	Image 4	Image 5	Image 6	Image 7	Image 8	Image 9	Image 10
5	94.70%	90.30%	99.10%	89.10%	94.70%	91.70%	98.10%	99.80%	91.60%	96.90%
10	85.30%	86.70%	86.20%	85.20%	89.30%	81.30%	81.90%	88.10%	81.20%	82.40%
15	83.30%	85.70%	78.30%	88.30%	80.30%	84.30%	88.10%	85.20%	82.10%	79.30%
20	74.70%	76.30%	69.50%	76.40%	79.70%	75.70%	71.20%	74.60%	71.90%	76.50%
25	73.80%	70.10%	69.30%	75.80%	75.80%	74.80%	76.60%	68.80%	74.80%	76.40%
30	70.90%	69.80%	68.20%	69.00%	66.90%	75.90%	72.30%	74.50%	67.40%	66.90%
35	60.70%	58.90%	63.80%	60.90%	57.70%	65.70%	57.70%	55.40%	65.90%	56.50%
40	54.40%	53.20%	54.80%	59.70%	54.40%	51.40%	57.20%	55.80%	59.70%	57.10%
45	40.70%	41.60%	36.50%	36.40%	43.70%	35.0%	37.80%	41.90%	45.40%	42.30%
50	34.50%	29.60%	34.30%	37.80%	33.50%	34.20%	38.10%	39.20%	35.70%	36.80%
55	28.90%	33.50%	26.80%	26.90%	23.90%	24.10%	29.90%	28.10%	30.50%	33.70%

with the detailed analysis of each picture done with the same method but with a parameter optimization by adjusting those belonging to each image.

In Figure 10 are compared the average values for effectiveness of each image resolution in function to the distance and the trend line representing the approximate behavior of the distance vs. effectiveness. This line corresponds to a lineal regression that meets the behavior of the obtained data (R^2 = 0.97 and R^2 = 0.985, respectively) and show that the type of behavior can be approximated to a lineal function where *X* is the distance and *Y* is the effectiveness percentage.

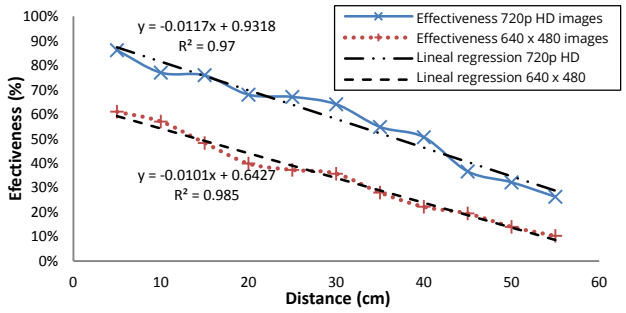

Figure 10. Comparative results of the effectiveness percentage in relation to the distance for the cameras with 640 x 480 and HD 720p resolution.

Based on the results obtained it can be deduced that the camera resolution HD 720p gives the best results for this application due to its superior effectiveness compared to the one of 640 x 480 (see Figure 10).

In Figure 11 is shown the result of the developed software, where the analysis of one of the testing images is observed, in this case one image at 5 cm of the crop taken with the HD 720p camera.

Figure 11. Result obtained with the developed software.

Economic benefits

A Drone like the one used in this study has a cruising speed of 5 m/s, whereas the human being walks, in average, 1m/s, which is a significant difference since at the end of a labor day (8 h) the Drone covers 14.4 Km more than the worker, which is an economic and social benefit. However the highest capacity battery for the AR has a maximum use time of 30 min and a total charge time of 4 h. the ARDrone 2.0 cost is approximately 500US$, each long duration battery costs 20US$ and its GPS module costs 150US$.

Conclusions

The use of recognition methods facilitates the analysis of pests in extensive cropping areas on a fast and assertive way.

The advantages of economic and social nature of this method are reflected in saving time of the field workers for revision of the crops, which implies reducing the physical effort and thus improve their quality of life.

Pest detection by image processing techniques is a fast process with economic advantages, especially to assist the agriculture sector in the monitoring of large areas of plantation. In the future it will be possible to improve some algorithms and adequate techniques such as adaptive filters to increase the performance of these algorithms and reduce dependence on external factors.

References

Barata, T.; and Pina, P. 2003. Morphological recognition of olive grove patterns. In: Perales F. J.; Campilho A. J.; Perez, N.; and Sanfeliu, A. Pattern recognition and image analysis. Mallorca. p. 89 - 96. Editorial Springer.

Bovik, A. C. 2005. Handbook of image and video processing, 2th. ed. London. Elsevier Academic Press.1384 p.

Etxeberria, J. A. 2010. Algoritmo de reconocimiento de forma y color para una plataforma robótica. Master thesis. Universidad del País Vasco. Department of Computational and Artificial Intelligence Science. In: http://www.ccia-kzaa.ehu.es/s0140con/es/contenidos/informacion/tesis_master/es_t_master/adjuntos/10jaristondo.pdf. Retrieved: July, 2013.

Fonterlz, J. O. 2013. *Begonia semperflorens*, Flor de Azúcar, Begonia siempre Florida. In: Plantas Villor, http://plantasvillor.es/begonia-

semperflorens-flor-de-azucar-begonia-siempre-florida/#.UhVWQJI9-zt. Retrieved: July, 2013.

Gedraite, E. S. and Hadad, M. 2011. Investigation on the effect of a Gaussian Blur in image filtering and segmentation. ELMAR Proceedings. p. 393 - 396.

Grbić, M.; Van Leeuwen, T.; Clark, R. M.; Rombauts, S.; Rouzé, P.; Grbić, V.; Osborne, E. J.; and Dermauw, W. 2011. The genome of *Tetranychus urticae* reveals herbivorous pest adaptations. Nature 479(7374):487 - 492.

Hendriks, L.; Cris, L.; Borgefors, G.; Strand. R. 2013. 11th International Symposium, 11th International Symposium, ISMM 2013, Uppsala, Sweden, May. p. 27 – 29.

Husin, Z. B.; Shakaff, A.; Aziz, A.; Farook, R. 2012. Feasibility study on plant chili disease detection using image processing techniques. Third Int. Conf. Intelligent Syst. Modelling and Simulation (ISMS). p. 291 - 296.

Yan, L.; Chunlei, X.; and Jang Myung, L. 2009. Vision-based pest detection and automatic spray of greenhouse plant. IEEE International Symposium on Industrial Electronics. p. 920 - 925.

Jin-liang, Y.; Yi-bo, G.; Liang-jun, M.; and Yi-Ping, Y. 2008. Scene text extraction based on HSL. International Symposium on Computer Science and Computational Technology. 2. p. 315 - 319.

Nixon, M. S. and Aguado, A. S. 2002. Feature extraction and image processing. 1th Ed. London. Newnes.

Noda, K.; Ezaki, N.; Takizawa, H.; Mizuno, S.; and Yamamoto, S. 2006. Detection of plant saplessness with image processing. International Joint Conference SICE-ICASE. p. 4856 - 4860.

Najman, L. and Talbot, H. 2010. Mathematical morphology: from theory to applications. ISTE-Wiley. 520 p.

Perkins, C. 2009. The blur & sharpen effects. In: the after effects illusionist. Boston. Focal Press. p. 43 - 84.

Shih, F. 2009. Image processing and mathematical morphology. CRC Press. p. 55 - 87.

Sun, D. W. 2012. Computer vision technology in the food and beverage industries. Elsevier. 208 p.

Wesolkowski, S.; Dony, R. D.; and Jernigan, M. E. 1999. Global color image segmentation strategies: Euclidean distance vs. vector angle. Neural Networks for Signal Processing. Proceedings of the IEEE Signal Processing Society Workshop. p. 419 – 428.